Simulation and Experimental Validation of a Silicon Photonics Ring Assisted Mach-Zehnder Interferometer Filter

Ana Clara Marques[1,2], Pedro Cabrita[3], Maria João Carvalhais[1], Catarina Novo[1,2], Mário Lima[1,2], Francisco Rodrigues[3] and António Teixeira[1,2,3]

[1]*Instituto de Telecomunicações, Universidade de Aveiro, Campus Universitário de Santiago, 3810-193 Aveiro, Portugal*

[2]*University of Aveiro, Aveiro, Portugal*

[3]*PICAdvanced AS, Ílhavo, Portugal*

Keywords: Ring-Assisted Mach-Zehnder Interferometer, Photonic Integrated Circuits, Optical Filters.

Abstract: This paper presents a comprehensive study on the simulation and laboratorial validation of ring assisted Mach-Zehnder interferometers (RAMZIs) for use as optical filters in demultiplexing systems in optical communication. The study explores the integration of a Mach-Zehnder interferometer (MZI) and an optical ring ressonator (ORR) to achieve a flat-top spectral response. The ORR and MZI are independently simulated before combining them into a RAMZI structure. The experimental results, obtained from a fabricated PIC on a SiOI platform, closely align with simulated spectrum, demonstrating the validity of the proposed model.

1 INTRODUCTION

Photonic integrated circuits (PICs) are considered a significant advancement in the field of telecommunications. Their capability of integrate many optical components such as filters, modulators, polarization elements, photodiodes or lasers into a single chip, combined with system flexibility, low cost and potential for large scale production, are some of the key characteristics that have driven extensive research into this technology over the past few years (Dong et al., 2014).

Optical selective bandpass filters are a special subgroup of components in optical transmission systems, particularly in wavelength-division multipplexing (WDM) systems, due to their ability to perform channel selection, demultiplexing and multichannel filtering (Kohli et al., 2021). These filters enable precise isolation of specific wavelengths or channels, ensuring efficient data transmission and reception over multiple channels simultaneously, thereby enhancing the overall performance of optical networks (Song et al., 2008).

Over the years, numerous optical components have been refined to perform as filters. Mach-Zehnder interferometer (MZI) stand out as a key example (Horst et al., 2013). It is a simple device based on a Y-splitter structure that divides the incoming light on the waveguide into two arms and then recombine the two signals allowing them to interfere and generate an output signal. The nature of this interference, whether constructive or destructive, depends on the optical path difference between the two arms (ΔL).

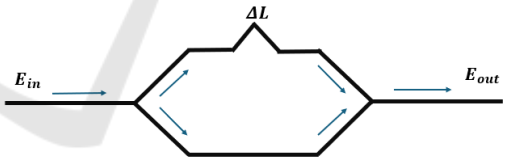

Figure 1: MZI scheme.

Although MZIs are fundamental components in Silicon Photonics (SiP), a single MZI is not capable of delivering a flat-top spectral response. To obtain a more rectangular shaped spectrum multiple stages, MZIs can be designed, although this approach increases the device footprint and complexity in design and fabrication processes. As an alternative, the design of ring assisted Mach-Zehnder interferometers (RAMZIs) appeared. This configuration offers a more box-like passband response compared to cascaded optical ring ressonators (ORRs) or MZIs with a simplified device sctructure (Sabri et al., 2024).

Marques, A. C., Cabrita, P., Carvalhais, M. J., Novo, C., Lima, M., Rodrigues, F. and Teixeira, A.
Simulation and Experimental Validation of a Silicon Photonics Ring Assisted Mach-Zehnder Interferometer Filter.
DOI: 10.5220/0013397500003902

In *Proceedings of the 13th International Conference on Photonics, Optics and Laser Technology (PHOTOPTICS 2025)*, pages 147-151
ISBN: 978-989-758-736-8; ISSN: 2184-4364

Conventionally this component consists of a basic MZI with a coupled ORR in its shorter arm.

A generic ring resonator consists of an optical waveguide which is looped back on itself, such that a resonance occurs when the optical path length of the resonator is exactly a whole number of wavelengths . In addition to that we have one straight waveguide that allows the access to the loop through a coupling mechanism. This specifically design is called all-pass filter and a scheme of the described component is shown in Figure 2 where the three main physical parameters of the device are represented as C_L for the coupling length, that refers to the straight path that separates the two halves of the ring, R for the radius of the ring and the gap, g, between the ring and the straight waveguide.

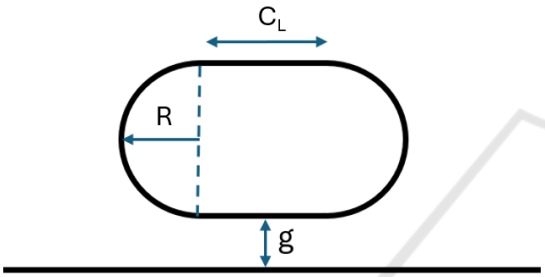

Figure 2: ORR scheme.

The addition of the ORR enables the RAMZI to exploit both the interference and resonance phenomena, making it suitable for applications requiring enhanced wavelength filtering or precision phase control, while retaining the basic functionality of the MZI. This straightforward configuration is known as a single-ring RAMZI, as showed in Figure 3. In recent years, various design modifications have been explored, including two or more cascading rings or parallel rings configurations (Kohli et al., 2021).

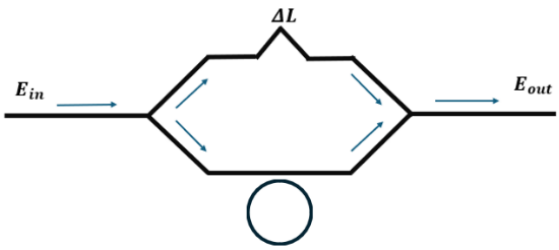

Figure 3: Single ring RAMZI scheme.

In this paper, for demonstration of the RAMZI working principle, we will present a model of simulation and experimental validation of the single ring RAMZI.

2 SIMULATION MODEL

This simulation process involves two steps. First the ORR and MZI are simulated independently to ensure that each component adheres to the required relationship between their Free Spectral Ranges (FSR), with the MZI's FSR being twice that of the ORR. Next, the two components are integrated to form a RAMZI.

2.1 ORR Simulation

The simulation of the ORRs for the design of RAMZI structures were carried out using the Variational Finite-Difference Time-Domain (varFDTD) solver in Ansys Lumerical. This solver provides an accurate representation of light propagation in planar integrated optical systems.

Simulating the rings is essential to determine the parameters required to calculate the Q-factor defined as the ratio between a resonant wavelength and its full width at half maximum (FWHM), as described in Equation 1. This Q-factor is then used to determine the coupling coefficient, k, between the straight waveguide and the ring, via Equation 2.

$$Q_{factor} = \frac{\lambda_{res}}{FWHM} \tag{1}$$

$$k = \sqrt{\left(\frac{n_g L\pi}{2Q\lambda}\right)^2 + 1} - \frac{n_g L\pi}{2Q\lambda} \tag{2}$$

Additionally, it is also essential to calculate the total length of the ORR using Equation 3.

$$L = 2\pi r + 2C_L \tag{3}$$

The calculated parameters, k and L, will serve as essential inputs for simulating the RAMZI.

The resulting spectrum of the simulated ORR with a radius of 5.5 µm, a coupling length of 1.5 µm and a gap of 200 nm, using a waveguide with an effective index, n_{ef}, of 2.5454, group index, n_g, of 3.9030, a width of 450 nm and a thickness of 120 nm is presented at Figure 4 corresponding to the expected response for this component compared to the reviewed literature (Bogaerts et al., 2012).

2.2 MZI Simulation

For simulating the MZI Lumerical INTERCONNECT was employed due to its

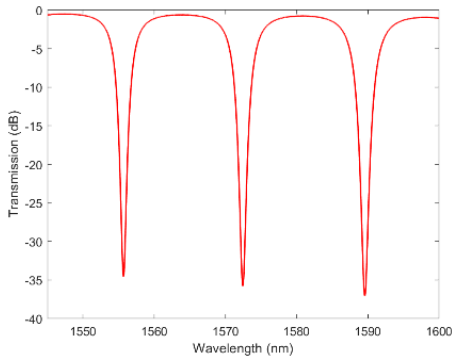

Figure 4: ORR spectrum.

capability to support block-based schematic designs. This software facilitates the creation and visualization of photonic circuits, enabling efficient simulation and analysis of the MZI architecture. Lumerical INTERCONNECT's framework allows easy parameter adjustments and comprehensive insights of the configuration's performance.

Figure 5 represents the MZI setup with the length of each parameter represented in µm. The input optical signal enters through the Y-branch splitter, which divides it into two paths, forming the two arms of the interferometer. In the upper arm, the signal propagates through two waveguide segments, one of them being 17.29µm, introducing a significant phase delay. In the lower arm, the signal travels through shorter waveguides. These two paths are then recombined at the directional coupler where the signals interfere. The output interference pattern is analysed by the Optical Network Analyzer.

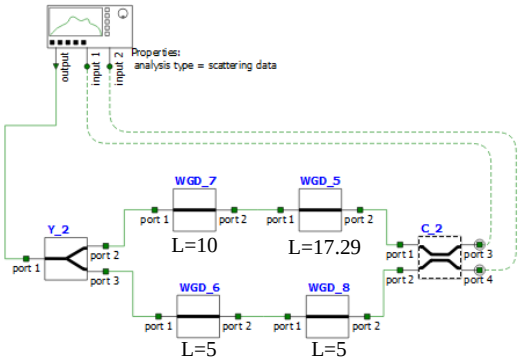

Figure 5: Block diagram of the simulated MZI.

The resultant spectra of this specific MZI is showed in Figure 6, showcasing the two output channels, and it also corresponds to the expected response for the respective component as seen in literature (Zheng et al., 2021).

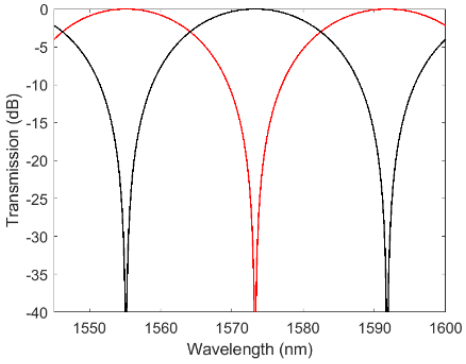

Figure 6: MZI spectrum.

2.3 RAMZI Simulation

The RAMZI simulation is essentially identical to the MZI, with the main difference being the addition of the ORR in the smaller arm as depicted in Figure 7. This ORR must follow the parameters established in the varFDTD simulation. To ensure it matches the original ring and maintains the same spectral response, the length and coupling coefficient calculated earlier are applied here.

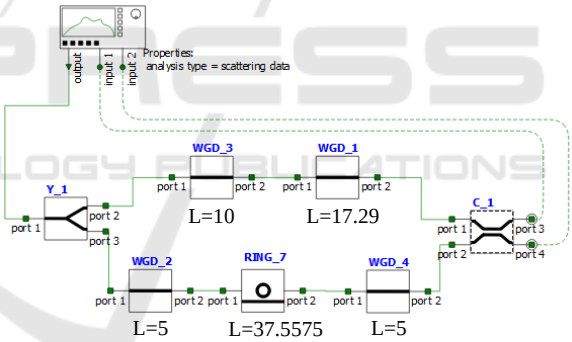

Figure 7: Block diagram of the simulated RAMZI.

Finally, the spectrum of the final component is depicted in Figure 8.

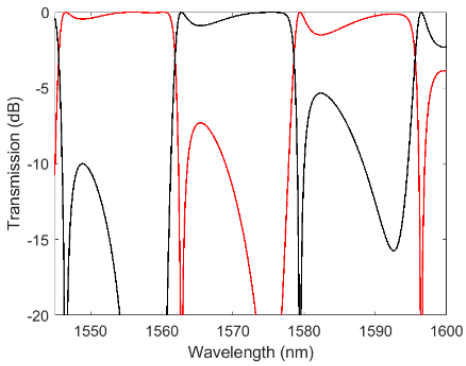

Figure 8: RAMZI spectrum.

As anticipated we can observe that the RAMZI exhibits a more rectangular response compared to the individual spectra of the ORR and MZI.

3 EXPERIMENTAL VALIDATION

To validate the simulation models, a laboratory test was done to compare the real and simulated spectrum. Both a RAMZI and an MZI from an existing PIC were tested, and the results were analysed in comparison with the simulated data.

The devices were designed using GDSfactory. The PIC was fabricated on a multi-project wafer from CORNERSTONE foundry and the stack is a SOI platform with rib waveguides.

The optical responses of the components were assessed by acquiring spectra at both ports of a MZI and a RAMZI using the experimental setup a depicted in Figure 9. In this setup, a C-L Band ASE Light Source provides the input light in the system. An Erbium Fiber amplifier(EDFA) is necessary to amplify the signal before it enters the PIC. Finally the output of the component is analysed with an Optical Spectrum Analyser (OSA).

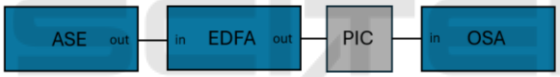

Figure 9: Experimental setup.

Figure 10 and Figure 11 show the experimental spectrums of a MZI and RAMZI respectively compared to its simulated spectrums.

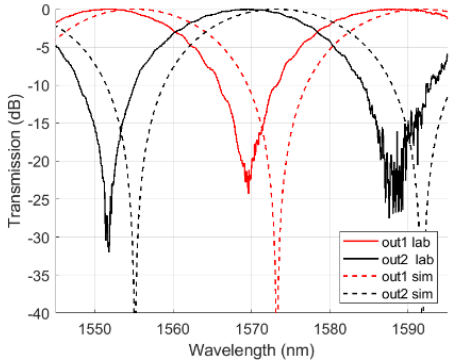

Figure 10: MZI experimental vs simulation.

By examining the results, we can conclude that, despite potential wavelength shift from the simulation possibly due to lithography differences between the simulated component and the fabricated one that will be explored in future work, the overall shape of the spectra aligns well. This consistency indicates that the simulation models are valid and are reliable for future analyses.

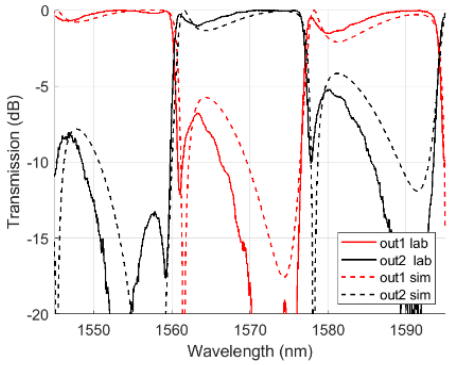

Figure 11: RAMZI experimental vs simulation.

4 CONCLUSIONS

In conclusion, this study successfully demonstrated the simulation and experimental validation of a RAMZI for optical filtering applications in photonic integrated circuits. By individually simulating the ORR and MZI and then integrating them into the RAMZI structure, we achieved a detailed understanding of their performance characteristics. The inclusion of the ORR in the MZI configuration enhanced the spectral response, offering a flatter passband and improved wavelength selectivity compared to a standard MZI. Experimental results from fabricated photonic chip showed good alignment with simulated spectra, validating the reliability of the simulation models despite minor deviations attributed to fabrication tolerances.

ACKNOWLEDGEMENTS

This work was supported by FCT – Fundação para a Ciência e Tecnologia, I.P. by project reference LA/P/0109/2020, and DOI identifier 10.54499/LA/P/0109/2020, https://doi.org/10.54499/UIDB/50008/2020

This work is supported by the European Regional Development Fund (FEDER), through the Competitiveness and Internationalization Operational Programme (COMPETE 2020) of the Portugal 2020 framework [Project POWER with Nr. 070365 (POCI-01-0247-FEDER-070365)] and Project SINO.

The University of Southampton and the UK Engineering and Physical Sciences Research Council (EPSRC) funded CORNERSTONE project (EP/L021129/1), CORNERSTONE 2 project

(EP/T019697/1) or CORNERSTONE 2.5 project (EP/W035995/1).

REFERENCES

Bogaerts, W., de Heyn, P., van Vaerenbergh, T., de Vos, K., Kumar Selvaraja, S., Claes, T., Dumon, P., Bienstman, P., van Thourhout, D., & Baets, R. (2012). Silicon microring resonators. In *Laser and Photonics Reviews* (Vol. 6, Issue 1, pp. 47–73). https://doi.org/10.1002/lpor.201100017

Dong, P., Chen, Y. K., Duan, G. H., & Neilson, D. T. (2014). Silicon photonic devices and integrated circuits. In *Nanophotonics* (Vol. 3, Issues 4–5, pp. 215–228). Walter de Gruyter GmbH. https://doi.org/10.1515/nanoph-2013-0023

Song, J., Fang, Q., Tao, S. H., Yu, M. B., Lo, G. Q., & Kwong, D. L. (2008). Passive ring-assisted Mach-Zehnder interleaver on silicon-on-insulator. *Optics express*, *16*(12), 8359–8365. https://doi.org/10.1364/oe.16.008359

Horst, F., Green, W. M. J., Assefa, S., Shank, S. M., Vlasov, Y. A., & Offrein, B. J. (2013). Cascaded Mach-Zehnder wavelength filters in silicon photonics for low loss and flat pass-band WDM (de-)multiplexing. *Optics Express*, *21*(10), 11652. https://doi.org/10.1364/oe.21.011652

Kohli, N., Sang, B., Nabki, F., & Menard, M. (2021). Tunable Bandpass Filter with Serially Coupled Ring Resonators Assisted MZI. *IEEE Photonics Journal*, *13*(4). https://doi.org/10.1109/JPHOT.2021.3103142

Sabri, L., Ahdab, R. El, Nabki, F., & Menard, M. (2024). Broadband SiN Interleaver with a Ring Assisted MZI Using a Tapered MMI Coupler. *IEEE Photonics Journal*, *16*(5). https://doi.org/10.1109/JPHOT.2024.3444825

Zheng, P., Xu, X., Hu, G., Zhang, R., Yun, B., & Cui, Y. (2021). Integrated Multi-Functional Optical Filter Based on a Self-Coupled Microring Resonator Assisted MZI Structure. *Journal of Lightwave Technology*, *39*(5), 1429–1437. https://doi.org/10.1109/JLT.2020.3037709